

Modification of surface states by alkali-metal adsorption and surface reconstruction: An inverse-photoemission study of Na/Ni(110)

N. Memmel, G. Rangelov, E. Bertel, and V. Dose

Max-Planck-Institut für Plasmaphysik—EURATOM Association, D-8046 Garching, Federal Republic of Germany

(Received 15 June 1990)

Unoccupied surface states were investigated on the reconstructed and unreconstructed Na/Ni(110) surface experimentally by inverse photoemission and theoretically by a phase-shift analysis in a nearly-free-electron model. For the (1×1) surface a downward shift of the surface states is observed as the Na coverage is increased up to monolayer completion. If reconstruction takes place, the direction of the energy shift is reversed and a surface state appears close to the Fermi level. In the theoretical model the alkali-metal-induced downshift is caused by the work-function decrease and by the additional phase shift of the surface-state wave function in the Na adlayer. On the reconstructed surface this effect is counteracted by the removal of Ni atoms from the topmost substrate layer. For near-monolayer coverages the surface states are shown to be closely related to the Na atomic wave functions.

I. INTRODUCTION

The adsorption of alkali metals on metal surfaces causes the appearance of adsorbate-induced surface states as demonstrated recently in photoemission and inverse-photoemission (IPE) spectroscopy.¹⁻⁴ These surface states are discussed in the literature in terms of essentially two different models. They have either been interpreted in the framework of a nearly-free-electron (NFE) model for surface states⁵⁻⁷ or as descending from the Bloch states of an unsupported two-dimensional alkali-metal layer.²⁻⁴ In the former model the energy position and k_{\parallel} dispersion of the surface states is strongly influenced by the substrate band gap, whereas advocates of the latter model usually liken the measured energies and dispersions to the band structure of the two-dimensional alkali-metal film.⁸ In order to further explore the merits of both models we chose to investigate a rather complex system, i.e., alkali-metal adsorption on reconstructing surfaces.

It is well known that the (110) surfaces of Au, Pt, and Ir show a (1×2) missing-row (MR) reconstruction. The clean (110) surfaces of Cu, Ag, Pd, and Ni, however, are unreconstructed but a (1×2) reconstruction can be induced by adsorption of small amounts of alkali metals. As was shown in recent experiments this reconstruction is also of the missing-row type.⁹⁻¹⁶ Since the transition is activated it does not occur on a sufficiently cold surface. This opens the possibility to study the Na-covered Ni(110) surface with and without surface reconstruction by choosing the proper sample temperature.

Models for the alkali-metal adsorption and surface reconstruction as proposed by Behm *et al.*¹⁶ are depicted in Fig. 1. On the (1×1) unreconstructed surface the alkali-metal atoms at low coverages adsorb disordered in the troughs of the (110) surface [Fig. 1(a)]. With increasing coverage the distance between the adatoms decreases until at monolayer coverage an ordered quasi-hexagonal

overlayer is formed [Fig. 1(b)]. On the (1×2) MR reconstructed surface, where each second row is absent, the alkali-metal atoms are located almost in the plane of the first Ni layer, whereas on the (1×1) surface they form an additional layer above the outermost Ni layer [Fig. 1(c)]. Near monolayer coverage the reconstruction is lifted and the quasi-hexagonal overlayer is formed as on the (1×1) surface.

As we wanted to investigate unoccupied surface states and their response to adsorption and reconstruction, we focused in our k -resolved IPE study on regions of k space where the substrate electronic structure shows large projected bulk band gaps. This is the case in the areas around the \bar{X} and the \bar{Y} points of the surface Brillouin zone. At the \bar{Y} point the gap extends from ≈ 0.1 to ≈ 6.1 eV above the Fermi level¹⁷ and contains two well-resolved surface states on clean Ni(110).^{18,19} We concen-

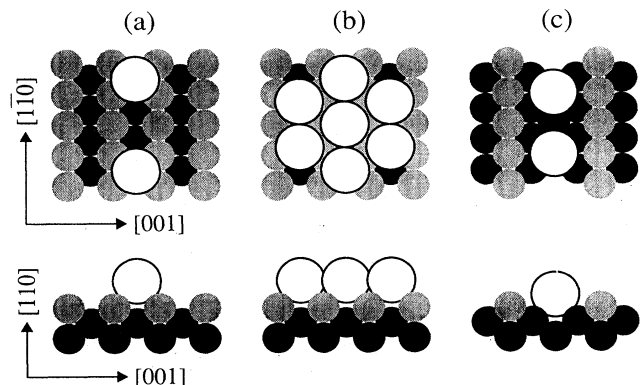


FIG. 1. Structure models for Na/Ni(110). (a) Low Na coverage on an unreconstructed surface. (b) Near monolayer coverage on an unreconstructed surface. (c) Intermediate Na coverage on a reconstructed surface.

trate in the following study on the behavior of the surface states in this band gap at the \bar{Y} point. As will be shown in this paper, Na adsorption as well as the Na-induced reconstruction of the Ni surface cause significant changes in the surface electronic structure. The experimental data are well described by the phase accumulation NFE model of surface states.

II. EXPERIMENT

The IPE facility is similar to that described in Ref. 20 and consists of an electrostatically focusing electron gun with a BaO cathode and two Geiger-Müller counters with iodine filling and SrF₂ windows resulting in a photon detection energy of 9.4 ± 0.2 eV.²¹ The two Geiger-Müller counters are mounted in the plane of incidence at fixed angles of 40° (counter 1) and 90° (counter 2) relative to the electron gun. The simultaneous use of two counters allows for partial polarization analysis, improves the energy resolution in cases of overlapping peaks from transitions with different emission characteristics,²⁰ and prevents overlooking a transition which does not emit photons into the direction of one of the counters. All surface and adsorbate-induced states reported below were seen with much higher intensity in counter 2 than in counter 1.

The angle of incidence ϑ can be changed by rotating the sample. The component k_{\parallel} of the wave vector k of the incoming electron parallel to the surface is given by

$$k_{\parallel} = [\hbar^2/2m(E_i - \Phi)]^{1/2} \sin \vartheta,$$

where E_i is the incident electron energy relative to the Fermi level and Φ the sample work function. The variation of the incident electron energy E_i , inherent to IPE spectroscopy in the isochromat mode, as well as the large work-function changes occurring upon alkali-metal adsorption will both alter k_{\parallel} if ϑ is kept constant. If we assume a final-state energy right at the Fermi level ($E_i = \hbar\omega = 9.4$ eV) a change in work function from ≈ 5 to ≈ 2 eV, as it occurs on alkali-metal adsorption, will change k_{\parallel} by as much as 30%. Therefore, spectra taken at a fixed angle of incidence for different alkali-metal coverages might show peak shifts which are solely due to the E versus k_{\parallel} dispersion of the observed transition. Similarly, for a given work function the relative change of k_{\parallel} as a function of the final-state energy between E_F and $E_F + 6.5$ eV amounts to even 50%. To avoid this undesirable complication the angle of incidence of the electrons was repeatedly adjusted while recording each of the spectra so as to obtain spectra for a given constant k_{\parallel} . All spectra shown were recorded near the \bar{Y} point of the surface Brillouin zone (SBZ) corresponding to angles of incidence from 30° up to 60° depending on the electron energy and sample work function.

Sodium was evaporated onto the surface from a well-outgassed commercial getter source (SAES Getters Inc.). Coverages were determined by a combination of thermal desorption spectroscopy, low-energy electron diffraction (LEED), and measurement of the Na-induced work-function change. The uncertainty of the coverage scale is estimated to $\pm 10\%$. The coverages are given throughout

this paper in fractions of a densely packed quasihexagonal monolayer, i.e., 1 ML = 8.1×10^{14} atoms/cm².²² As there are 1.15×10^{15} Ni atoms in the ideally terminated substrate surface layer this corresponds to 0.7 ML Na in the conventional definition with respect to the substrate atoms.

Two different techniques were used to prepare the Na overlayers. In preparation mode 1, as it will be called henceforth, different amounts of Na were dosed onto the sample which was kept at 100 K in order to inhibit surface reconstruction. Up to a coverage of 0.4 ML no long-range order of the adsorbate layer could be observed by LEED, while further adsorption of Na produced extra LEED spots due to the formation of a quasihexagonal overlayer.

In preparation mode 2, approximately two monolayers of Na were initially evaporated onto the Ni crystal at 100 K. Then part of the Na was thermally desorbed by annealing the sample. The temperatures required to produce the desired coverages ranged from 380 K for a full monolayer to ≈ 800 K for zero coverage. Fractional-order spots could clearly be observed by LEED for coverages between 0.15 and 0.80 ML, indicating that reconstruction had taken place. At higher coverages the reconstruction was lifted and the LEED pattern of the quasihexagonal Na monolayer appeared. The sequence of LEED patterns is virtually identical to that reported by Gerlach and Rhodin²² for Na adsorbed on Ni(110) at 300 K.

For both preparation modes the measurements reported below were performed at a sample temperature of ≈ 100 K. At this temperature the long-range order is significantly improved as compared to room temperature.¹⁶ Furthermore, the intensity of IPE transitions is usually larger at low temperatures.²³

III. CALCULATIONS

In order to account for the observed changes in surface-state energies upon Na adsorption and surface reconstruction we have calculated the energies of surface and adsorbate-induced states using a phase-shift analysis originally proposed by Echenique and Pendry²⁴ and successfully applied by Smith and co-workers^{19,25-27} as well as Lindgren and Wallden⁵⁻⁷ to predict surface-state energies on clean and adsorbate-covered Cu and Ni surfaces. A NFE two-band model is used to obtain the wave function in the crystal and the surface barrier is described by a planar-averaged one-dimensional potential. Due to these severe approximations the calculation is expected to correctly predict trends in surface-state energies and dispersions but not to exactly reproduce the whole experimental data set. As the trends do not strongly depend on the details of the model the choice of the actual form of the potential used to describe the adsorbed layer or the surface reconstruction is not very critical. Following Lindgren and Wallden⁵⁻⁷ we model a monolayer of alkali metal on the surface by a region of constant potential with thickness d_{Na} and depth V_{Na} between the crystal and barrier potential. The potential is schematically de-

pictured in Fig. 2. In the region $z < z_0$ where the two-band approximation is used the corresponding Fourier component of the crystal potential is drawn. Beyond z_0 the potential is chosen to have the constant value V_0 of the Ni bulk inner potential.²⁴ At a point z_C the potential jumps discontinuously to the value V_{Na} . The flat potential region of depth V_{Na} and width d_{Na} represents the Na overlayer. At $z_B = z_C + d_{\text{Na}}$ the potential is continuously joined to the image potential.

For modeling coverages below one monolayer Lindgren and Wallden⁵ have suggested to keep the width of the Na potential well fixed and to vary the inner potential proportional to $(\Theta_{\text{Na}})^{2/3}$. Alternatively one could keep the potential depth fixed and change the thickness d_{Na} of the potential representing the adsorbate.²⁸ While the first method is usually used in self-consistent jellium calculations, in the simple model used here only the second one yields a reasonable potential in the zero-coverage limit. Therefore we choose the second alternative for modeling submonolayer coverages. Clearly the use of a planar-averaged one-dimensional potential is a debatable approximation at low coverages, but it may be justified *a posteriori* in the present case because the model nicely reproduces the evolution of the adsorbate-induced states out of the clean surface states, as it is observed in the experiment. It should also be noted that despite similar simplifications the jellium model yields a rather satisfying description of the work-function changes even at small alkali-metal coverages.²⁸

The parameters V_0 , V_G , and V_{Na} are determined by the bulk band structure of the respective metals in the following way: The inner potential V_0 and the Fourier component V_G representing the Ni crystal are obtained from the NFE description of the spin-averaged bulk L_2 - L_1 band gap.¹⁷ This yields values of $V_0 = -6.2$ eV (relative to E_F) and $V_G = 3.2$ eV, respectively. The potential V_{Na} of the Na potential well is set to the value of the Na bulk inner potential which is -3.2 eV (relative to E_F). The remaining three parameters z_0 , z_C , and z_B are subject to the following constraints: For the thickness of the adsorbate layer $d_{\text{Na}} = z_B - z_C$ at monolayer coverage we take the vertical distance between the Na atoms and the

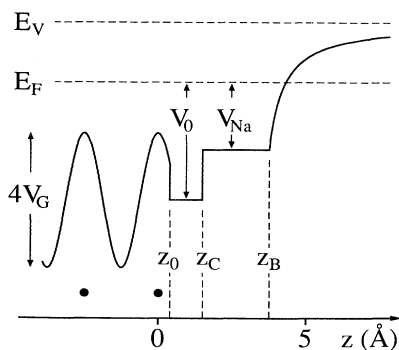


FIG. 2. Schematic of the model potential for the Na/Ni(110) surface. V_G refers to the Fourier component of the potential which opens the gap of width $2V_G$ at the \bar{Y} point. The other parameters are discussed in the text.

outermost Ni plane. In a hard-sphere model this yields 2.25 Å which is about 25% less than the distance between two close-packed hexagonal Na layers and accounts for the fact that sodium is adsorbed on the open Ni(110) surface. This choice of d_{Na} may appear somewhat arbitrary, but as we are only analyzing trends, the particular choice of d_{Na} has no relevance for the conclusions drawn below. Furthermore, for the unreconstructed surface we follow Ref. 24 and take z_0 to be the position of the outermost Ni atoms which are located at $z=0$. Thus z_C is left as the only adjustable parameter in the model potential. It is adjusted to fit the measured surface-state energies in the zero-coverage limit ($\Theta_{\text{Na}}=0$). By this procedure we obtain for $d_{\text{Ni}} = z_C - z_0$ a value of 1.11 Å. This may be compared to 0.9 Å obtained by Smith, Chen, and Weinert²⁷ who used a slightly different model for the surface potential barrier.

The (1×2) MR reconstruction can be incorporated into the present model if the 50% reduction of the surface layer density is appropriately accounted for. In analogy to the Na overlayer this can be modeled by a shortening of the Ni potential region by half a Ni(110) interlayer spacing, i.e., z_0 is shifted inwards by 0.63 Å. In order to obtain the correct behavior in the limiting cases of no change in Ni atom density and complete Ni monolayer removal, respectively, the constant potential region V_0 between z_0 and z_C has to be independent of the Ni surface atom density. The adsorption of sodium is described as on the unreconstructed surface.

IV. RESULTS AND DISCUSSION

Figure 3(a) shows a series of IPE spectra recorded with counter 2 at the \bar{Y} point of the Ni(110) SBZ for different Na coverages which were obtained using preparation mode 1 as described above. The three structures *A*, *B*, and *C* in the spectrum of the clean surface were already observed by Goldmann *et al.*¹⁸ and are interpreted as follows. Peak *A* is due to a transition into the unoccupied part of the Ni *d* band. At the \bar{Y} point the corresponding final-state energy is very close to the gap edge and therefore Garrett and Smith¹⁹ suggested that emission from a surface state could also contribute to peak *A*. Peak *B*, clearly located in the projected bulk band gap, is attributed to a crystal-induced surface state. The weak structure *C* near the upper edge of the band gap is assigned to the first image potential state.

Upon Na adsorption peak *B* loses intensity and is shifted continuously from 2.3 eV above E_F (clean surface) to 0.8 eV (completion of the Na monolayer). The image state *C* is rapidly quenched by Na adsorption. At 0.4 ML an adsorbate-induced structure appears at ≈ 4 eV above E_F which increases in intensity, shifts down, and splits in energy as more sodium is deposited.

A similar set of spectra is shown in Fig. 3(b), but this time the Na layers were prepared using preparation mode 2. Quite abrupt changes in peak energies and intensities occur between $\Theta_{\text{Na}}=0.1$ and 0.3 ML, and also between $\Theta_{\text{Na}}=0.8$ and 0.9 ML. These coverages coincide with the coverages at which LEED shows the appearance and disappearance, respectively, of the reconstruction-

induced fractional-order spots. Therefore we attribute the observed abrupt changes in the IPE spectra to reconstruction-induced changes in the surface electronic structure. This conclusion is supported by a comparison with the spectra of the unreconstructed surface [Fig. 3(a)]. At low ($\Theta_{\text{Na}} < 0.15$ ML) and high ($\Theta_{\text{Na}} > 0.9$ ML) coverages the spectra are essentially identical, whereas in the intermediate-coverage range the spectra are quite different, the most pronounced difference being a rapid upward shift of peak *B* at coverages near 0.2 ML on the reconstructed surface in marked contrast to the continuous downward shift on the unreconstructed surface. We reported a very similar behavior for Ag(110) where the surface shows the same kind of reconstruction upon Na adsorption.^{29,30}

A close inspection of the data reveals small differences even at low coverages ($\Theta_{\text{Na}} \approx 0.1$ ML), where LEED shows a (1×1) pattern in both cases. While the surface state on the cold Na-dosed surface is slightly lower than on the clean surface, it is shifted to ≈ 0.1 -eV higher energies on the annealed surface indicating a local rearrangement of the surface.^{11,16} The image state, which was quenched at low coverages on the cold (1×1) surface, can be followed nicely on the annealed surface indicating that the surface is better ordered in the latter case.

A close up of the spectra of counter 2 (solid circles) and counter 1 (open circles) in the energy range near E_F is

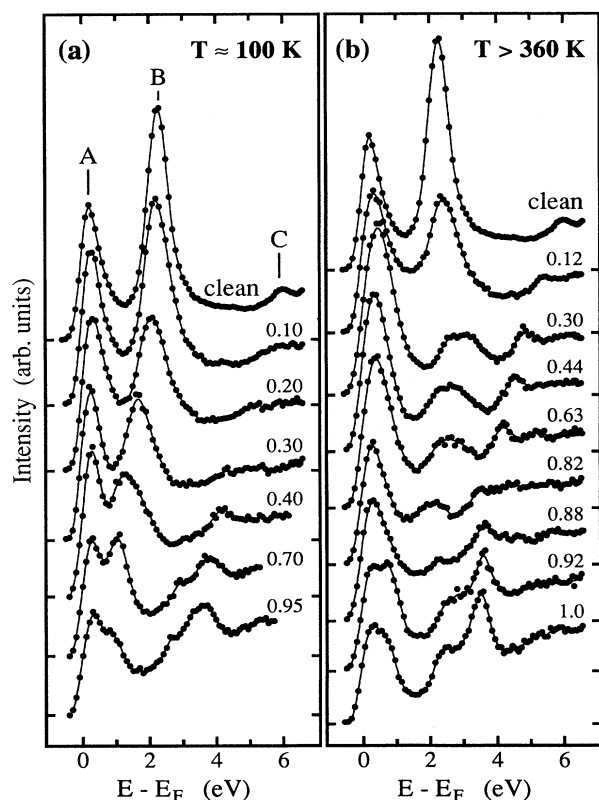


FIG. 3. IPE spectra of Na/Ni(110) recorded at the \bar{Y} point. Temperatures given in (a) and (b) relate to different preparation techniques as described in the text. The Na coverage is given in fractional monolayers for each spectrum.

shown in Figs. 4(a) and 4(b) for the cold and annealed surface, respectively. The energy position of peak *A* as determined on the clean surface is indicated by a thin vertical line. The position of the peak maximum is the same in both counters and nearly constant for all Na coverages on the (1×1) unreconstructed surface [Fig. 4(a)]. This also holds true for the peak maximum observed in counter 1 for the annealed surface, while in counter 2 a shift of the peak maximum to higher energies accompanied by a drastic intensity increase occurs between coverages of $\Theta_{\text{Na}} = 0.12$ and 0.30 ML [Fig. 4(b)]. Clearly two transitions (with different emission characteristics) contribute to this structure around the coverage of 0.30 ML. Therefore we conclude that the Na-induced reconstruction of the surface causes a peak to appear at the high-energy side of peak *A*. Upon further adsorption of Na the difference between the spectra in the two counters decreases until at $\Theta_{\text{Na}} \approx 0.8$ –0.9 ML both spectra are nearly identical. A shift of the reconstruction-induced state towards the Fermi level or a decrease in emission strength or both can be responsible for such a behavior. Near monolayer coverage, where the reconstruction is lifted again, a peak appears in counter 2 at ≈ 0.8 eV, which by comparison with the spectra of the unannealed surface

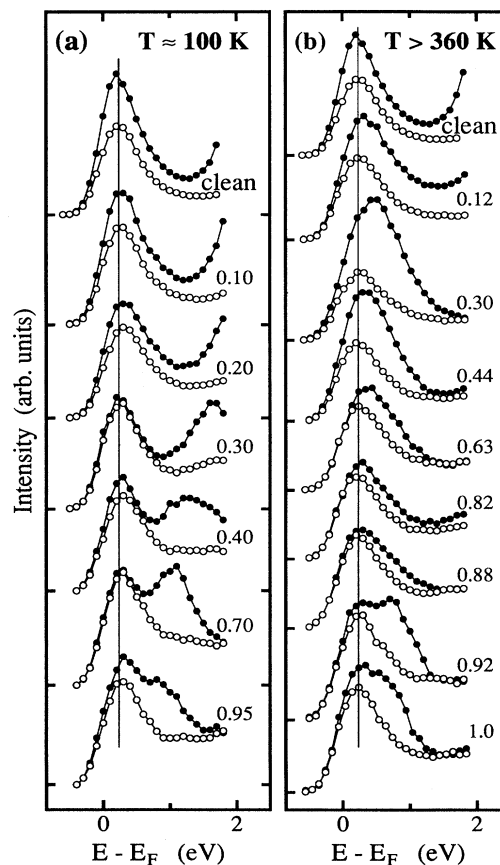


FIG. 4. Detailed view of the IPE spectra shown in Fig. 3. Solid and open circles refer to different photon detection angles of 90° and 40° relative to the incident electron beam. The thin vertical line marks the energy position of the transition observed on the clean surface.

[Figs. 3(a) and 4(a)], can be identified as the downshifted peak *B*.

The surface reconstruction is also reflected in the work-function measurements (Fig. 5). On the reconstructed surface the Na-induced work-function change is always smaller than on the (1×1) surface, the differences being as large as 0.8 eV. As is pointed out in Ref. 11, this is a consequence of the sodium atoms being much closer to the metal on the reconstructed surface (they almost merge into the first Ni layer—see Fig. 1). Thereby the alkali-metal-induced surface dipole moment is reduced and a smaller work function change results. These differences occur already at the lowest coverages ($\Theta_{\text{Na}} < 0.1$ ML) where no extra LEED spots can be observed and they are interpreted as being due to a local rearrangement of the surface in this coverage range.^{11,16}

We now turn to a theoretical description of the experimental data. In Fig. 6(a) surface-state energies obtained from a phase-shift analysis (dashed lines) for an unreconstructed surface are compared with the experimental data points (open symbols). The calculations reflect the observed behavior very well: The pronounced downward shift of peak *B* with increasing coverage as well as the appearance of two adsorbate-induced states between 2 and 4 eV for the Na monolayer are nicely reproduced. As can be seen in Fig. 6(a), the peak at ≈ 2.5 eV evolves out of the 6-eV surface state seen at point \bar{Y} on the clean surface.¹⁸ This state is the lowest of a whole Rydberg series of image states on the clean surface, which, however, are not resolved in IPE. The surface state appearing at ≈ 3.7 eV for the Na monolayer on Ni(110) descends from the next higher image state of the clean Ni(110) surface.

In the present model the downward shift of all surface states is caused by two effects. The first one is the increase of the width d_{Na} of the Na potential well with in-

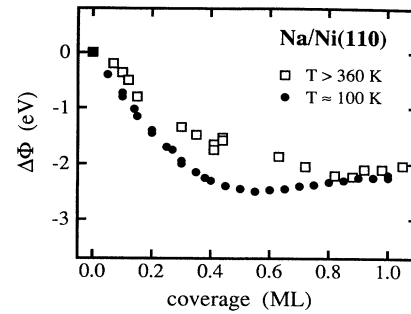


FIG. 5. Na-induced work-function change resulting from different preparation techniques (see text).

creasing coverage, the second one the alkali-metal-induced work-function decrease. The latter effect, however, is only relevant for states close to the vacuum level and has little influence on lower-lying levels such as peak *B*.³¹ The quantum numbers attached to the right of the calculated lines in Fig. 6 reflect the node structure and symmetry of the surface states according to the convention used by Smith.²⁵ “+” and “−” denote the even and odd symmetry of the wave function with respect to the family of mirror planes perpendicular to the $[001]$ direction containing the origin, and therefore, also the Ni atoms of the topmost substrate layer. Note that the reverse-symmetry assignment applies for mirror planes containing the Na atoms because the Na atoms are located in the troughs halfway between two adjacent Ni rows.

Near zero coverage the calculations predict a strong downward shift for peak *B*, whereas the initial energy shift observed in the experiment is very small. This may indicate that the simple model used here breaks down in

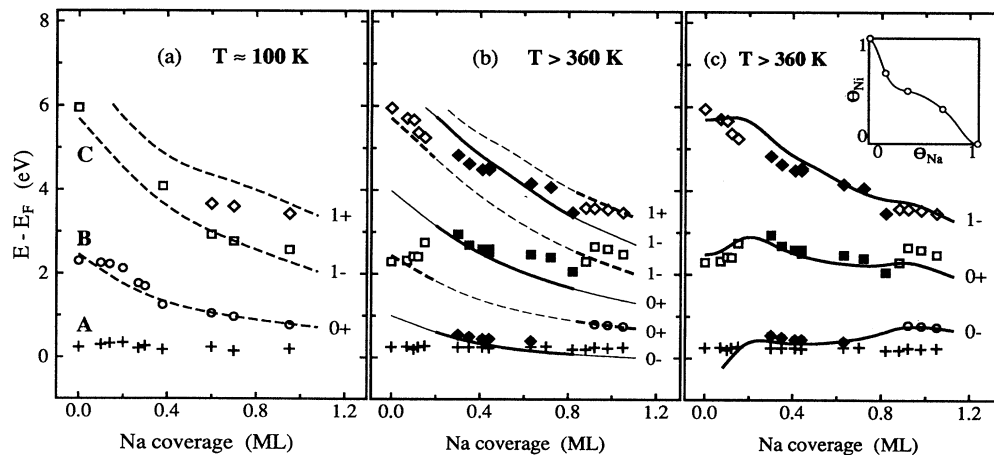


FIG. 6. Comparison of experimental (symbols) and calculated (lines) results for the surface-state energies as a function of Na coverage for different preparation techniques. Open (solid) symbols are used for the experimental data points on the unreconstructed (reconstructed) surface. Different symbols at the same coverage denote different transitions. Dashed (solid) lines show results from calculations assuming an unreconstructed (missing-row reconstructed) surface. The solid lines shown in (b) are calculated assuming a (1×2) MR reconstruction. The solid lines in (c) are calculated assuming a sequence of $(1 \times n)$ MR reconstructions as determined by Behm *et al.* (ref. 16). The corresponding relative Ni vs Na coverage on the reconstructed surface is shown as an inset in (c). Data points are from Ref. 16; the interpolation is discussed in the text.

the very-low-coverage range.

Experimental and theoretical results for the annealed surface are compared in Fig. 6(b). Two sets of calculations have been performed. The dashed lines show the behavior of the surface-state energies when the surface reconstruction is taken into account only via the different work function change (Fig. 5) and the model potential for the Ni substrate is not altered. In the second set of calculations (solid lines) the Ni potential is modified in order to account for the reduced Ni density on the (1×2) reconstructed surface (see Sec. III). The first set of calculations, where the change in surface atom density is neglected, agrees with the experimental data near zero and monolayer coverage, but completely fails to describe the energy position of peak *B* in the coverage range from 0.2 up to 0.9 ML where reconstruction is observed by LEED. For this coverage range, however, the second set of calculations, where reconstruction (viz. Ni atom density reduction) is taken into account, yields a fairly good agreement between the experimental and theoretical results. In particular the observed drastic upward shift of peak *B* around coverages of 0.2 ML and the further shift at 0.9 ML is nicely borne out by the calculations and is shown to result from the surface reconstruction. In Fig. 6(b) this corresponds to transitions from dashed to solid lines at $\Theta_{\text{Na}} \approx 0.2$ ML and from solid to dashed lines at $\Theta_{\text{Na}} \approx 0.9$ ML, respectively. The calculations also correctly predict the appearance of an additional surface state close to E_F . A comparison of the two sets of calculations shows that the 50% reduction of the Ni density in the topmost substrate layer occurring upon reconstruction causes an upward shift of all surface states. The shift is most pronounced for the lower-lying "crystal-induced" surface states. Consequently the surface state appearing at $E_F + 0.5$ eV on the reconstructed surface derives from an upward-shifted surface state of the unreconstructed surface which in our calculations is placed below E_F . Using a similar calculational scheme but a slightly different model potential Garrett and Smith¹⁹ placed this surface state just above E_F and suggested that it contributes to peak *A* in the spectrum of the clean surface.

The strong shift of the surface states caused by changes in the topmost Ni layer density, as it is predicted by the calculations and experimentally verified by the present data, bears another highly interesting implication. It has long been an open question whether the (1×2) reconstruction of the (110) surfaces of fcc metals is only a displacive reconstruction with no change in surface-atom density, such as, for example, a pairing-row reconstruction or if it is a true reconstruction involving density changes as in the case of the MR reconstruction. The present results demonstrate that these two types of reconstruction can be discriminated by measuring the reconstruction-induced surface-state energy shifts. A (1×2) pairing-row reconstruction can be induced on Ni(110) by hydrogen adsorption at low temperatures and in this case we actually observed a continuous down shift of the surface states,³² analogous to the present case of Na adsorption on the unreconstructed surface. This is to be expected because in both cases the substrate surface atom density is unchanged.

When comparing the experimental and theoretical results in Fig. 6(b) one should bear in mind that the present discussion of the (1×2) MR reconstruction is based on a simplified phase diagram. At low (high) Na coverages $(1 \times n)$ reconstructions are observed, where every *n*th Ni row is missing (left in place).¹⁶ From the structure models proposed by Behm *et al.*¹⁶ one can extract the Ni and Na concentrations in the topmost layer for the (1×3) and the (1×2) reconstructed surface. If it is assumed that the reconstruction, viz., the reduction in Ni atom density, starts already at very low coverages,^{11,16} and if the smooth evolution of the relative Ni concentration during the transition from the first to the second Na monolayer is taken into account, one obtains the diagram for the relative Ni versus Na coverages which is shown as an inset in Fig. 6(c). If these relative coverages are used as input for the present model calculations the pattern of the experimental surface-state shifts is faithfully reproduced throughout the whole coverage range, as it is illustrated in Fig. 6(c). A comparison between Figs. 6(b) and 6(c) shows for the Na monolayer a seemingly contrasting symmetry assignment of the surface states. This is a consequence of the model used here, because the reconstruction is assumed to proceed by stepwise removal of the topmost Ni layer. The lifting of the reconstruction at monolayer coverage is equivalent with the completion of this process, i.e., with the removal of the last Ni atoms from the topmost substrate layer. Thus the former second Ni layer becomes the outermost substrate layer. The Ni atoms in this surface layer are shifted by half a Ni-Ni distance in the [001] direction with respect to the Ni atoms of the original unreconstructed surface. Consequently, the reflection symmetry with respect to the origin—which is designated by the symmetry labels—is changed. But the symmetry with respect to a mirror plane containing the Ni atoms of the actual outermost layer remains the same.

Figure 7 displays the squared wave functions of the surface states and resonances for the clean surface and the surface covered by a full Na monolayer. The calculated energies relative to E_F are also indicated. For the $n = 0+$ crystal-induced surface state on the clean surface the maximum value of $|\psi|^2$ occurs just outside the surface. The maximum shifts further out if one proceeds to the $n = 1-$ and $n = 1+$ image states as it is expected. After adsorption of a monolayer of sodium the probability distributions have still non-negligible tails into the substrate but substantial parts of the wave functions are located inside the sodium overlayer. Therefore these states are mixed substrate/adsorbate states and should be termed adsorbate-induced or overlayer states⁷ instead of surface states. Obviously a projection of the wave functions onto atomic orbitals of the appropriate symmetry yields substantial overlap. All states labeled with + are odd with respect to the Na atoms in the sense explained above, so only Na p_y -, d_{xy} -, and d_{yz} -like orbitals (where *x* denotes the $[\bar{1}10]$, *y* the [001], and *z* the [110] direction) can contribute to these states, while Na s , p_x , p_z , etc. character can be mixed into the states labeled with -. Since the $n = 0+$ state is ≈ 2 eV below the vacuum level the Na *d* states are not expected to play an important role

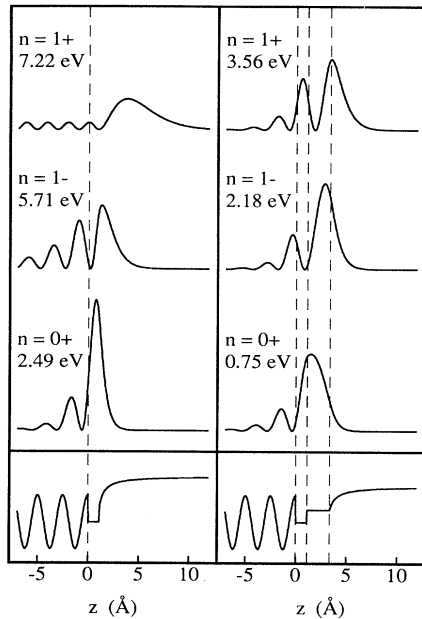


FIG. 7. Upper panels: plot of $|\psi|^2$ at the \bar{Y} point for various surface states and resonances of the clean Ni(110) surface (left) and for the surface covered with a full monolayer of sodium (right). The calculated energies relative to E_F and the quantum numbers n are given. + and - denote even and odd symmetry with respect to the Ni surface atoms. Lower panels: Schematic diagram of the potentials used to describe the clean and Na-covered surface. Dashed lines indicate the position of the outermost Ni atoms and the range of the Na potential.

in this case. Therefore the Na admixture to this state is mostly of p_y character, whereas Na s , p_x , p_z , and possibly some d states are mixed into the $n=1-$ state. This analysis is consistent with band-structure calculations for an unsupported hexagonal Na monolayer⁸ which at the \bar{M} point of the hexagonal Na Brillouin zone [corresponding to the \bar{Y} point of the Ni(110) SBZ] place the lowest odd band below the even state.

The $n=1+$ and the $n=1-$ state of the Na-covered Ni(110) surface which evolve from the symmetric and antisymmetric $n=1$ image state of the clean surface can no longer be considered as "image states," since these states also exist—however, at slightly higher energies—if a simple step potential instead of the long-range image potential is used to terminate the sodium overlayer. The reason is that the Na layer causes the surface potential well to be sufficiently long ranged in order to sustain two additional bound states.

The apparent success of the NFE phase-analysis model of surface states in the present context of alkali-metal adsorption and surface reconstruction as well as in the previously investigated case of hydrogen adsorption³² raises the question to what extent this model may be applied in the description of adsorbate-induced states. The NFE character of the model implies that it should be used only for surface states in an sp band gap. In Ni the lower gap edge at the \bar{Y} point merges into the d bands, but the

shape of the gap is only weakly distorted by the d bands. Thus the model yields still qualitatively correct predictions. Furthermore, the use of a constant potential for modeling the adlayer and the expansion of the wave functions into only a few plane waves, inherent to the NFE approximation, imposes a constraint on the adsorbates to which this kind of phase analysis may be applied: It is essential that they cause only a weakly varying pseudopotential for electrons in the energy range under consideration. Therefore the model works well for hydrogen and the alkali metals. We also believe that it may profitably be applied to the description of sp metal adsorbates. It remains questionable whether the model can successfully be applied to, for example, chalcogenides and halogenides. For molecular adsorbates such as CO it obviously fails. The attempt to describe the oxygen-induced empty states on a Cu(110) surface²⁶ by this model became controversial, because the calculations did not reproduce the correct dispersion for an oxygen-derived state. Apparently tight-binding calculations proved to be superior in this respect.³³ With our present knowledge we are not able to make a definitive stand in this controversy, but we would like to point out that the limitations of the present model are yet to be explored.

A final comment concerns the role of the Ni d bands. The Ni d bands are not explicitly included into the present calculations. Indirectly they affect the position of the band gap at the \bar{Y} point which in turn is taken into account by an appropriate choice of the bulk potential V_0 . Any d mixture into the surface-state wave functions, however, is completely neglected in the calculations. The good overall agreement between the calculations and the experimental data leads to the conclusion that the Ni d bands play only a minor role in the formation of the overlayer states. Thus it is the interaction with the substrate sp bands which determines the character of these unoccupied alkali-metal-induced states.

V. SUMMARY

The adsorption of Na on Ni(110) was studied by k-resolved IPE. Alkali-metal adsorption causes a (1×2) reconstruction of the (110) surface. The reconstruction is activated and can therefore be suppressed by keeping the sample always at low temperature. The behavior of unoccupied surface states in the band gap around the \bar{Y} point was investigated for both cases. Na adsorption causes a strong downward shift of the existing and the appearance of new surface states in the case of the non-reconstructed surface. On the reconstructed surface the behavior of the surface states is more complex. A rapid upward shift of the crystal-induced surface states at low coverages is followed by a slight down shift as the Na concentration increases on the reconstructed surface. Close to monolayer coverage the reconstruction is lifted and again an up shift of the surface states is observed. Model calculations have been carried out which allow a qualitative understanding of these energy shifts. The substrate band structure was described by a NFE two-band

approximation, the adlayer by a constant inner potential, and the vacuum barrier by a truncated image potential. Increasing Na coverage was simulated by increasing the thickness of the corresponding constant potential range from zero to the atomic layer distance at monolayer coverage. A phase-shift analysis yields then immediately the observed down shift of the surface states with increasing coverage. When reconstruction takes place the increasing phase shift caused by the Na adlayer is counteracted by the reduction of the number density of the Ni atoms in the topmost layer which results in an upward shift. Close to monolayer completion the reconstruction is lifted and the surface-state energies are again the same as on the nonreconstructed surface. The present data and their consistent interpretation in a comparatively simple model

demonstrate that the measurement of unoccupied surface states provides a viable method for discriminating different types of reconstruction.

Finally it is shown that an analysis of the symmetry and the probability distribution of surface states clarifies their relation to the alkali-metal atomic wave functions but simultaneously reveals their mixed substrate-adsorbate character. The Ni *d* bands are not involved in the formation of the observed alkali-metal overlayer states.

ACKNOWLEDGMENTS

We thank M. L. Hirschinger for her valuable help in carrying out the experiments.

- ¹S. A. Lindgren and L. Wallden, *Solid State Commun.* **28**, 283 (1978); **34**, 671 (1980).
- ²K. Horn, A. Hohlfeld, J. Somers, Th. Linden, P. Hollins, and A. M. Bradshaw, *Phys. Rev. Lett.* **61**, 2488 (1989).
- ³W. Jacob, E. Bertel, and V. Dose, *Phys. Rev. B* **35**, 5910 (1987).
- ⁴D. Heskett, K. H. Frank, E. E. Koch, and H. J. Freund, *Phys. Rev. B* **36**, 1276 (1987); K. H. Frank, H. J. Sagner, and D. Heskett, *Phys. Rev. B* **40**, 2767 (1989).
- ⁵S. A. Lindgren and L. Wallden, *Phys. Rev. B* **38**, 3060 (1988).
- ⁶S. A. Lindgren and L. Wallden, *Phys. Rev. Lett.* **59**, 3003 (1987); **61**, 2894 (1988); *Phys. Rev. B* **38**, 10044 (1988); *Surf. Sci.* **211/212**, 394 (1989).
- ⁷S. A. Lindgren and L. Wallden, in *Physics and Chemistry of Alkali Metal Adsorption*, edited by H. P. Bonzel, A. M. Bradshaw, and G. Ertl (Elsevier, Amsterdam, 1989), 101.
- ⁸E. Wimmer, *J. Phys. F* **13**, 2313 (1983).
- ⁹B. E. Hayden, K. C. Prince, P. J. Davie, G. Paolucci, and A. M. Bradshaw, *Solid State Commun.* **48**, 325 (1983).
- ¹⁰S. M. Francis and N. V. Richardson, *Surf. Sci.* **152/153**, 63 (1985).
- ¹¹R. Döhl-Oelze, E. M. Stuve, and J. K. Sass, *Solid State Commun.* **57**, 323 (1986).
- ¹²J. W. M. Frenken, R. L. Krans, J. F. van der Veen, E. Holub-Krappe, and K. Horn, *Phys. Rev. Lett.* **59**, 2307 (1987).
- ¹³C. J. Barnes, M. Q. Ding, M. Lindroos, R. D. Diehl, and D. A. King, *Surf. Sci.* **162**, 59 (1985); C. J. Barnes, M. Lindroos, and D. A. King, *Surf. Sci.* **201**, 108 (1988); C. J. Barnes, M. Lindroos, D. J. Holmes, and D. A. King, *ibid.* **219**, 143 (1989); in *Physics and Chemistry of Alkali Metal Adsorption*, edited by H. P. Bonzel, A. M. Bradshaw, and G. Ertl (Elsevier, Amsterdam, 1989), p. 129.
- ¹⁴M. Copel, W. R. Graham, T. Gustafsson, and S. Yalisove, *Solid State Commun.* **54**, 695 (1985).
- ¹⁵W. C. Fan and A. Ignatiev, *J. Vac. Sci. Technol. A* **7**, 2115 (1989).
- ¹⁶R. J. Behm, D. K. Flynn, K. D. Jamison, G. Ertl, and P. A. Thiel, *Phys. Rev. B* **36**, 9267 (1987); R. J. Behm, in *Physics and Chemistry of Alkali Metal Adsorption*, edited by H. P. Bonzel, A. M. Bradshaw, and G. Ertl (Elsevier, Amsterdam, 1989), p. 111.
- ¹⁷H. Eckardt and L. Fritsche, *J. Phys. F* **17**, 925 (1987).
- ¹⁸A. Goldmann, M. Donath, W. Altmann, and V. Dose, *Phys. Rev. B* **32**, 837 (1985).
- ¹⁹R. F. Garrett and N. V. Smith, *Phys. Rev. B* **33**, 3740 (1986).
- ²⁰M. Donath, M. Glöbl, B. Senftinger, and V. Dose, *Solid State Commun.* **60**, 237 (1986); M. Donath, V. Dose, K. Ertl, and U. Kolac, *Phys. Rev. B* **41**, 5509 (1990).
- ²¹V. Dose, Th. Fauster, and R. Schneider, *Appl. Phys. A* **40**, 203 (1986).
- ²²R. L. Gerlach and T. N. Rhodin, *Surf. Sci.* **17**, 32 (1969).
- ²³R. Schneider, H. Dürr, Th. Fauster, and V. Dose, *Phys. Rev. B* **42**, 1638 (1990).
- ²⁴P. M. Echenique and J. B. Pendry, *J. Phys. C* **11**, 2065 (1978).
- ²⁵N. V. Smith, *Phys. Rev. B* **32**, 3549 (1985).
- ²⁶C. T. Chen and N. V. Smith, *Phys. Rev. B* **40**, 7487 (1989).
- ²⁷N. V. Smith, C. T. Chen, and M. Weinert, *Phys. Rev. B* **40**, 7565 (1989).
- ²⁸N. D. Lang, *Phys. Rev. B* **4**, 4234 (1971).
- ²⁹N. Memmel, W. Jacob, E. Bertel, and V. Dose (to be published).
- ³⁰N. Memmel, G. Rangelov, E. Bertel, and V. Dose, *Surf. Sci.* (to be published).
- ³¹Note that the perpendicular energy has to be considered, which at the \bar{Y} point is ≈ 3 eV lower than the actual electronic energy.
- ³²G. Rangelov, N. Memmel, E. Bertel, and V. Dose, *Surf. Sci.* **236**, 250 (1990).
- ³³L. H. Tjeng, M. B. J. Meinders, and G. A. Sawatzky, *Surf. Sci.* **233**, 163 (1990).

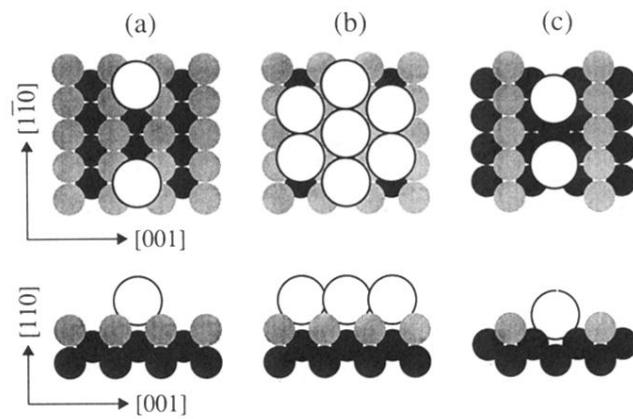


FIG. 1. Structure models for Na/Ni(110). (a) Low Na coverage on an unreconstructed surface. (b) Near monolayer coverage on an unreconstructed surface. (c) Intermediate Na coverage on a reconstructed surface.